Polymer Chemistry

Paper

Polymerization Induced Self-Assembly: Tuning of Morphology using Ionic Strength and pH†

Received 00th January 20xx,
Accepted 00th January 20xx

DOI: 10.1039/x0xx00000x

www.rsc.org/

Dewen Zhou,[a] Siming Dong,[a] Rhiannon P. Kuchel,[b] Sebastien Perrier,[c,d] and Per B. Zetterlund*[a]

Investigations of RAFT dispersion polymerization-induced self-assembly (PISA) of 2-hydroxypropyl methacrylate (HPMA) in water/methanol at 60 °C using a cationically charged macroRAFT agent as stabilizer block, namely P(*N,N*-diethylaminoethyl methacrylate)-*stat*-poly((ethylene glycol) methyl ether methacrylate) (PDEAEMA-*stat*-PEGMA), have been conducted with a view to tune particle morphologies by manipulation of the pH and the ionic strength. Above the LCST (45 °C) of (PDEAEMA-*stat*-PEGMA), the system can only be conducted as a dispersion polymerization at sufficiently low pH such that the stabilizer block is sufficiently protonated to ensure solubility in the continuous phase. It is demonstrated (reported in the form of an extensive morphology diagram) that a range of morphologies including spherical particles, rods and vesicles can be accessed by adjustment of the pH (via addition of HCl) and the ionic strength (via the concentration of NaCl). A decrease in the charge density of the coronal stabilizer layer via an increase in pH (less protonation) shifts the system towards higher order morphologies. At a given pH, an increase in ionic strength leads to more extensive charge screening, thus allowing formation of higher order morphologies.

Introduction

Polymerization-induced self-assembly (PISA)[1-9] via reversible addition-fragmentation chain transfer (RAFT) polymerization has emerged as a convenient method for synthesis of polymer nanoparticles of a wide range of different morphologies. The method is based on in situ formation of an amphiphilic diblock copolymer, followed by self-assembly when the second block reaches sufficient length. Compared to traditional ways of preparing such nano-objects via a gradual decrease in concentration of a common solvent by addition of a selective solvent,[10-14] PISA presents various advantages such as ease of implementation, not time-consuming, and perhaps most importantly the ability to access high solids contents (up to 50%). PISA has been implemented as both emulsion polymerization [15-23] and dispersion polymerization,[24-29] most commonly the latter in recent years. Various parameters influence the morphology of the nanoparticles formed during PISA: (*i*) the relative lengths of the hydrophilic and the hydrophobic blocks;[24, 26, 29-31] (*ii*) the interactions between each block and the solvent;[26, 32] (*iii*) the monomer concentration (in dispersion polymerization),[24, 26, 29, 30] and (*iv*) in the case of aqueous formulations, the pH value and salt concentration.[15, 16, 23, 25, 28, 33, 34] In recent work,[35] we demonstrated how CO_2 can be used to tune the particle morphology in dispersion PISA.

Polymeric nanoparticles comprising block copolymers with cationic,[28, 34, 36-38] anionic[25, 39, 40] and zwitterionic[41, 42] character have been synthesised via PISA. In both dispersion and emulsion-based PISA systems, it has been shown that the morphology is influenced by the charge density of the solvophilic block – if the charge density is too high, only spheres can form due to the strong repulsive forces between the chains on decreasing the curvature of the interface between the core and the continuous phase. Higher order morphologies such as rods and vesicles have a lower degree of curvature, thus bringing the solvophilic chains in closer proximity, thereby creating stronger repulsive interactions in case of charged chains, making their formation less favoured thermodynamically. It has however been demonstrated that higher order morphologies can be obtained by use of various strategies to reduce the charge density within the coronal stabiliser layer: (*i*) incorporation of a non-ionic comonomer into the solvophilic block; (*ii*) use of a mixture of an ionic macroRAFT and a non-ionic macroRAFT; (*iii*) addition of salt to achieve electrostatic screening of the charges.[15, 16]

The tertiary amine group of the monomer *N,N*-diethylaminoethyl methacrylate (DEAEMA) allows control of the extent of positive charge via the extent of protonation as dictated by the pH via addition of e.g. HCl at pH values below its pKa (~8.4).[43] This property renders DEAEMA attractive for controllable and tunable block copolymer self-assembly. Cunningham and coworkers have reported the use of DEAEMA as solvophilic block in NMP emulsion polymerization exploiting in situ formed amphiphilic block copolymer self-assembly as nucleation mechanism to generate spherical particles.[44-46] Lansalot and Carlmark[38] conducted RAFT emulsion polymerization based on the PISA process to obtain spherical particles comprising P(DMAEMA-*stat*-MAA)-*b*-PMMA, and Armes and coworkers reported synthesis of spherical particles of poly(2-(dimethylamino)ethyl methacrylate-*b*-stearyl methacrylate) (PDMAEMA-*b*-PSMA) *via* RAFT dispersion polymerization in ethanol.[37] Despite the potential of tuning the charge density of P(DMAEMA) by adjustment of the pH, to the best of our knowledge there are no precedents of exploiting this property to tune the PISA particle morphology beyond spherical particles.

[a] Centre for Advanced Macromolecular Design (CAMD), School of Chemical Engineering, The University of New South Wales, Sydney, NSW 2052, Australia Tel: +61 2 9385 4331; Fax:+61 2 9385 6250; E-mail: p.zetterlund@unsw.edu.au
[b] Mark Wainwright Analytical Centre, University of New South Wales, Sydney, NSW 2052, Australia.
[c] Department of Chemistry, The University of Warwick, Gibbet Hill, Coventry, CV4 7AL, United Kingdom.
[d] Faculty of Pharmacy and Pharmaceutical Sciences, Monash University, 381 Royal Parade, Parkville, VIC 3052, Australia

† Electronic Supplementary Information (ESI) available: See DOI: 10.1039/x0xx00000x

In the present work, we have conducted RAFT dispersion PISA of 2-hydroxypropyl methacrylate (HPMA) in water/methanol using a macroRAFT agent prepared from copolymerization of DEAEMA and poly(ethylene glycol) methyl ether methacrylate (M_n = 475 g mol^{-1})(PEGMA). It is noteworthy that this PISA process is only possible if the solvophilic block is sufficiently protonated (otherwise it is insoluble in the medium), *i.e.* by proper adjustment of the pH to be sufficiently low. It is demonstrated that by tuning the pH and/or the ionic strength, the morphology of the obtained nanoparticles can be readily tuned to access spherical particles, worm/rods or vesicles for a given recipe.

Experimental

Materials

N,N-Diethylaminoethyl methacrylate (DEAEMA, 99% Sigma-Aldrich) and poly(ethylene glycol) methacrylate (PEGMA, M_n = 475 g mol^{-1}; Sigma-Aldrich) were passed through basic alumina to remove the inhibitor. 2,2′-Azobisisobutyronitrile (AIBN) was recrystallized twice from methanol. HPMA (Sigma-Aldrich), comprising approximately 75 mol% 2-hydroxypropyl methacrylate and 25 mol% 2-hydroxyisopropyl methacrylate, was purified by silica column chromatography to reduce the content of dimethacrylate impurity,[24] and used within 4 weeks. 4-Cyano-4-(phenylcarbonothioylthio) pentanoic acid (CPADB, >97% Sigma Aldrich), hydrochloric acid (HCl, 32% RCl Labscan; diluted to 0.5 mol L^{-1}), 4,4′-azobis(4-cyanovaleric acid) (ACVA, ≥99% Sigma Aldrich), sodium chloride (NaCl, Univar), toluene (99.5%, Univar) and *N,N*-dimethylacetamide (DMAc, 99.9%, Sigma-Aldrich), methanol (Huntsman Corporation Australia PTY Limited), deuterated dimethyl sulfoxide-d_6 (DMSO-d_6; Cambridge Isotope Laboratories) were used as received. Deionized (DI) water was obtained by a Milli-Q reverse osmosis system with a resistivity of 19.6 mΩ cm^{-1}.

Synthesis of P(DEAEMA-*stat*-PEGMA) macroRAFT.

In a typical experiment, a glass vial was charged with DEAEMA (1 g, 5.398 mmol), PEGMA (641 mg, 1.349 mmol), CPADB (31.4 mg, 0.112 mmol), AIBN (3.6 mg, 0.0219 mmol), and 1,3,5-trioxane (34.0 mg, 0.377 mmol) as internal standard for determination of the monomer conversion by ^{1}H NMR in toluene (4.5 ml). The solution was poured into a septum-sealed vial, purged for 30 min with nitrogen in an ice-water bath and heated to 65 ^{o}C in a thermostated oil bath under magnetic stirring. The polymerisation was quenched after 18 h by immersion of the vial in ice/water. The individual monomer conversions were determined by ^{1}H NMR spectroscopy in DMSO by the relative integration of the protons of 1,3,5-trioxane and the vinylic protons of both monomers (overall conversion = 62%). Based on the assumption that all RAFT agents initially present correspond to a polymer chain after polymerization, it was calculated that the macroRAFT has the composition P(DEAEMA$_{30}$-*stat*-PEGMA$_7$). DMAc GPC (vs poly(methyl methacrylate) calibration standards) yielded M_n = 7,900 g mol^{-1} and $Đ$ = 1.12. The macroRAFT was purified by dialysis against methanol for 24 h. Note that a slightly different macroRAFT, P(DEAEMA$_{35}$-*stat*-PEGMA$_8$) (M_n = 9,300 g mol^{-1} and $Đ$ = 1.09), was employed for the experiments shown in Fig. 1.

RAFT dispersion polymerisation.

In a typical aqueous dispersion polymerisation, HPMA (100 mg, 0.694 mmol; 16.4% w/w), 4,4'-azobis (4-cyanopentanoic acid) (ACVA, 0.864 mg, 0.00308 mmol), NaCl (11.69 mg, 0.2 mmol) and macroRAFT agent (12.33 mg, 0.00154 mmol) were dissolved in water/methanol mixture (500 mg, 20 vol% MeOH). The pH of the resulting solution was adjusted as required by addition of aqueous HCl (pH/ION meter S220 (SevenCompact)), followed by nitrogen purging for 15 min. Polymerization was commenced by submerging the glass vial in a preheated oil bath at 60 ^{o}C for 2 h. The macroRAFT: initiator molar ratio was fixed at 1:2 in all cases.

Polymer Characterisation

1H NMR Spectroscopy All NMR spectra were recorded using a 400 MHz Bruker Avance-400 spectrometer in dimethyl sulfoxide-d_6 (DMSO-d_6).

Gel Permeation Chromatography (GPC). Molecular weights and molecular weight distributions (MWDs) were determined by GPC employing a Shimadzu modular system with dimethylacetamide containing 0.03% w/v LiBr and 0.05% w/v 2,6-dibutyl-4-methylphenol (BHT) as eluent at 50 ^{o}C at a flow rate of 1.0 mL/min with injection volume of 100 µL. The GPC was equipped with a DGU-12A solvent degasser, a LC-10AT pump, a CTO-10A column oven and an RID-10A refractive index detector, and a Polymer Laboratories 5.0 µm bead-size guard column (50×7.5 mm) followed by four linear Styragel columns. The system was calibrated against poly(methyl methacrylate) standards ranging from 500 to 10^5 g mol^{-1}.

Dynamic Light Scattering (DLS). DLS measurements were performed using a Malvern Zetasizer Nano Series running DTS software and using a 4mW He-Ne laser operating at a wavelength of 633nm and an avalanche photodiode (APD) detector. The scattered light was detected at an angle of 173^o at 25 °C. It is noted that DLS theory is based on spherical objects – the DLS data in this work thus correspond to a spherical object having the same diffusion characteristics as the object in question (which in this study may be a sphere or a non-spherical object). The diameters reported are as such only semi-quantitative in nature.

Transmission Electron Microscopy (TEM). The size and morphologies of the nanoparticles were observed using a JEOL1400 TEM at an accelerating voltage of 100 kV. The raw nanoparticle dispersion was diluted with water or water/MeOH (same continuous phase used as in the polymerization) in the concentration range of 0.2-0.5 mol/L. One drop of the diluted sample was deposited onto a copper grid (ProSciTech). 2% Uranyl Acetate solution as negative staining was applied for all samples.

Results and Discussion

Overall considerations.

The focus of this work has been to elucidate to what extent the morphology of polymer particles prepared by PISA can be tuned via the ionic strength and the pH. Aqueous RAFT dispersion polymerization systems with a stabilizer block based on DEAEMA and a core-forming block of HPMA were investigated. Poly(DEAEMA) is insoluble in water at temperatures above its LCST of 45 °C unless in its protonated form at sufficiently low pH. Poly(HPMA) is insoluble in water, although its monomer exhibits moderately high water solubility, and thus fulfils the criteria for dispersion PISA as reported previously.[29] Earlier work has demonstrated that using a polyelectrolyte as the sole stabiliser block only gives access to spherical morphologies as a result of the strong electrostatic repulsion between the charged stabiliser chains.[15] Excessive electrostatic repulsion prevents the morphological transition from spheres to higher order morphologies such as rods and vesicles – the lower curvature of rods/vesicles brings the stabilizing chains in closer proximity, which becomes energetically too costly at high charge densities of the chains.[33, 47] Thus, the charge density of the DEAEMA chains was in the present work

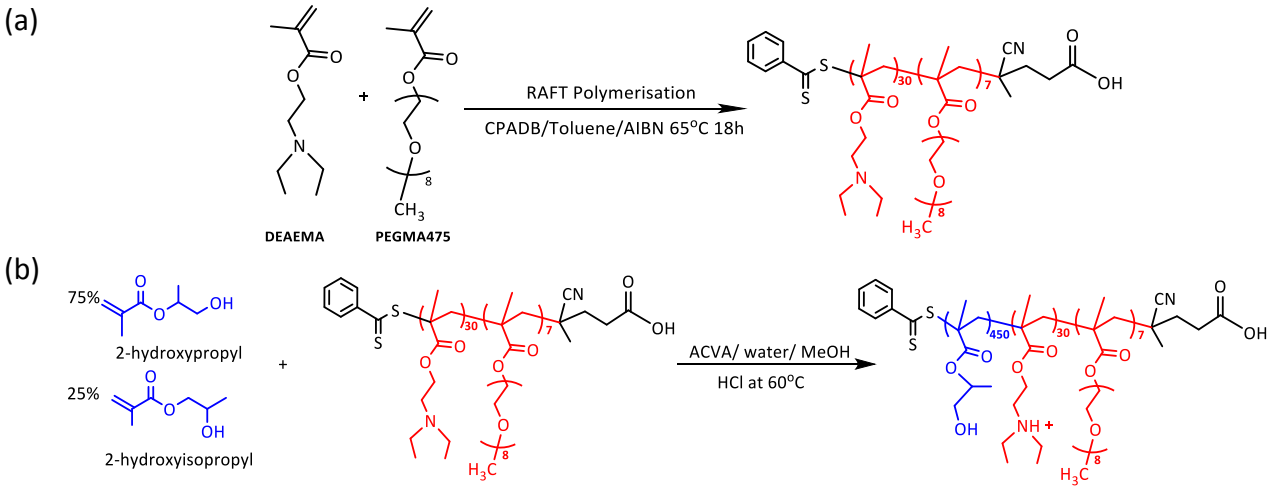

Scheme 1. (a) Synthesis of P(DEAEMA$_{30}$-*stat*-PEGMA$_7$) macroRAFT via RAFT polymerization and (b) RAFT dispersion polymerization (PISA) of HPMA using P(DEAEMA$_{30}$-*stat*-PEGMA$_7$) macroRAFT.

reduced by introduction of PEGMA units. RAFT solution copolymerisation was conducted in toluene at 65 °C using [CPADB]:[AIBN] = 5:1 (Scheme 1a), yielding P(DEAEMA$_{30}$-*stat*-PEGMA$_7$) according to ^{1}H NMR (GPC: M_n = 7,900 g mol^{-1}; $Đ$ = 1.12). The general PISA procedure entailed the use of the P(DEAEMA$_{30}$-*stat*-PEGMA$_7$) macroRAFT agent with HPMA at 16.4% w/w monomer at 60 °C for 2h in water. ACVA was used as radical initiator at [macroRAFT]:[ACVA] = 1:2 (Scheme 1b). This ratio may seem high – however, based on k_d (ACVA; water; 60 °C) = 4.93×10^{-6} s^{-1}, only 3.5% of the ACVA decomposes during the polymerization. In all cases, ^{1}H NMR data confirmed that the monomer conversions were above 95%, while DMAc GPC analysis (PMMA calibration) indicated $Đ$ < 1.3.

Effect of adding salt on morphology.

PISA was conducted in water at pH = 7 using P(DEAEMA$_{35}$-*stat*-PEGMA$_8$) targeting a degree of polymerization (DP$_n$) of 500 at full conversion of HPMA. Under these conditions, in the absence of added salt, rather polydisperse spherical particles (~65 nm) were obtained (Fig. 1a). Given the significant length of the PHPMA block, this indicates that the presence of 19 mol% PEGMA in the stabilizer block is not sufficient to reduce the strong repulsive electrostatic forces between DEAEMA chains in the coronal layer, thus preventing formation of higher order morphologies. In the presence of 0.6 M NaCl, considerably larger spherical nanoparticles (~85 nm) of narrower size distribution were obtained (Fig. 1b). The charge screening afforded by NaCl enables the system to form larger spherical micelles via an increase in the aggregation number (N_{agg}), thus leading to a decrease in the overall interfacial area between the core and the solvent (water) of the system (and thus overall interfacial energy).[33] Similar effects have been observed previously by Armes and coworkers for RAFT aqueous dispersion PISA involving a cationic electrolyte as corona and HPMA as core forming monomer.[28]

Effect of adding methanol on morphology.

In order to access higher order morphologies such as rods and vesicles, the medium was changed from pure water to 20% v/v methanol/water. Armes and coworkers[26] have previously demonstrated that when using high molecular weight PHPMA as the second block in RAFT dispersion PISA, addition of a cosolvent can shift the morphologies towards rods/vesicles by virtue of its effect on the mobility of the chains in the core (reduction of the effective T_g). The addition of methanol (0.6 M NaCl) did indeed lead to higher order morphologies as evidenced by TEM imaging - pure rods were obtained (Fig. 1c). In the case of pure water as medium, not all HPMA is soluble at the start of the polymerization – the excess would be present as monomer droplets. As such, the system should

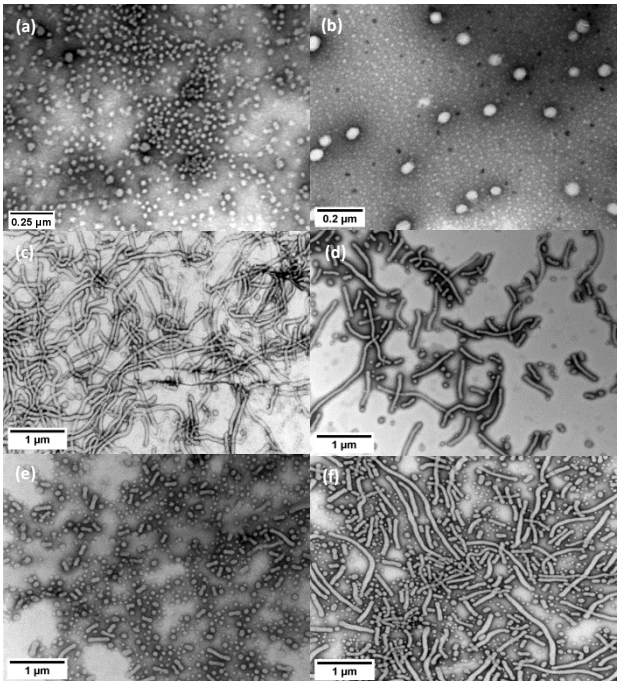

Fig. 1 TEM images for dispersion PISA of HPMA (16.4% w/w; target DP$_n$ = 500 using P(DEAEMA$_{35}$-*stat*-PEGMA$_8$) macroRAFT at 60 °C at various conditions. (a) and (b) were conducted at pH = 7; (a) No NaCl in pure water; (b) 0.6 M NaCl in pure water (black dots are NaCl crystals; very small white dots are not particles but a feature of the grid); (c)-(f) were conducted with 0.6 M NaCl in water/methanol (4:1) at (c) pH = 7, (d) pH = 6, (e) pH = 5.5, (f) pH = 4. All HPMA monomer conversions > 95%.

be classified as an emulsion polymerization as opposed to a dispersion polymerization. In the presence of 20% v/v methanol, the system is fully homogeneous at the beginning of polymerization (Fig. S1).

Effect of adding acid on morphology.

Lowering the pH value leads to partial protonation of the amine group of the DEAEMA units of the hydrophilic block. As a result, the charge density of the PDEAEMA block increases and the overall repulsion among the corona chains increases. An increase in the charge density of the stabilizer block generally shifts the morphologies towards entities with greater curvature, *i.e.* in the direction vesicles-rods-spherical micelles.[15, 47]

PISA was conducted in water: methanol (20% v/v methanol) in the presence of 0.6 M NaCl at 60 °C using P(DEAEMA$_{35}$-co-PEGMA$_8$) targeting DP$_n$ = 500 at full conversion at various pH values by addition of HCl. As the pH decreased from 7 to 6, the lengths of the rods decreased markedly, and at pH 5.5 a mixture of very short rods and spherical micelles was obtained. The pKa of PDEAEMA is ~7.4, thus when the pH value is decreased from 7 (Fig. 1c) to 6 (Fig. 1d) towards 5.5 (Fig. 1e), the repulsion forces between chains increases with the increasing degree of protonation. The larger the repulsion force, the more likely spherical morphology is formed. It is interesting that when the pH was reduced further to 4, a morphology transition back towards longer rods occurred. This reversal in the trend can most likely be explained by the excess HCl acting as a salt, thus screening the effect of the cationic charge. A further consideration is that a reduction in pH leads to a reduced degree of ionization of the single terminal carboxylic acid group located at the α-end of the stabilizer block, thus making it less water soluble. Reducing the solubility of the stabilizer block can be

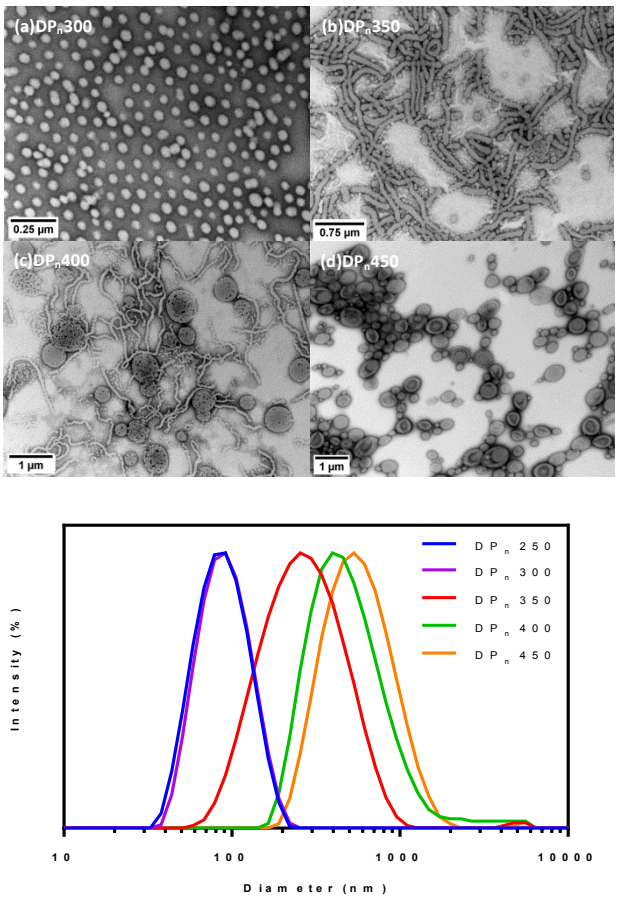

Fig. 3 Representative TEM images and DLS size distributions for dispersion PISA of HPMA (16.4% w/w) using P(DEAEMA$_{30}$-*stat*-PEGMA$_7$) macroRAFT at 60 °C targeting different values of final DP$_n$ of HPMA block of (a) 300, (b) 350, (c) 400, and (d) 450. All HPMA monomer conversions > 95%.

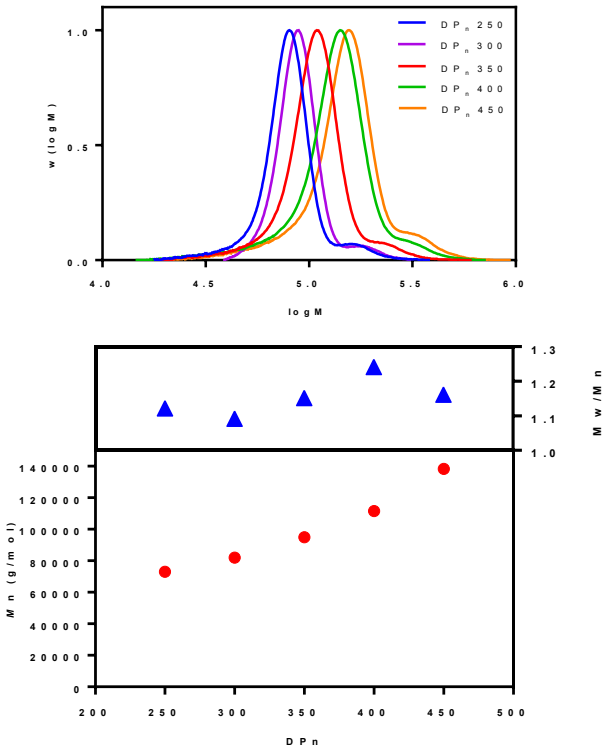

Fig. 2 Molecular weight distributions for dispersion PISA of HPMA (16.4% w/w) using P(DEAEMA$_{30}$-*stat*-PEGMA$_7$) macroRAFT at 60 °C targeting different values of final DP$_n$ of HPMA block as indicated. All HPMA monomer conversions > 95%.

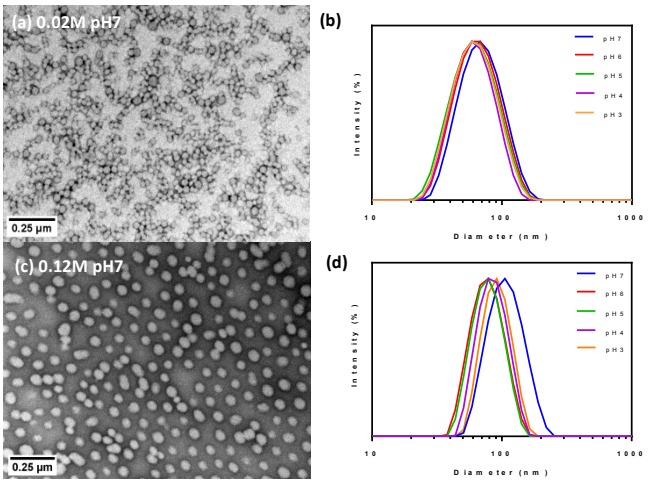

Fig. 4 Representative TEM images (at pH7) and DLS size distributions for dispersion PISA of HPMA (16.4% w/w) using P(DEAEMA$_{30}$-*stat*-PEGMA$_7$) macroRAFT at 60 °C targeting different pH values with the ionic strength of (a) 0.02M and (c) 0.12M. All HPMA monomer conversions > 95%.

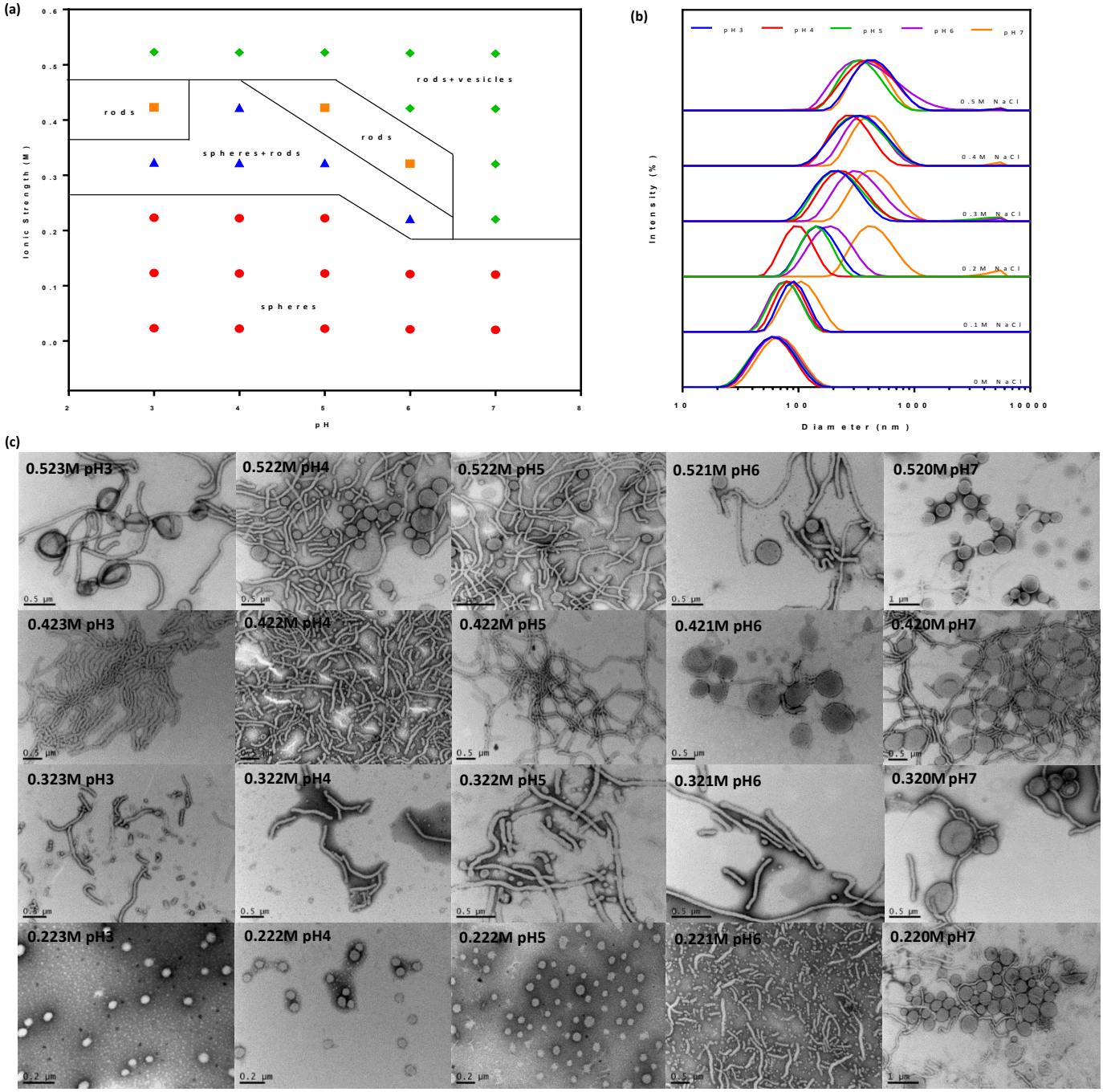

Fig. 5 (a) Detailed phase diagram constructed for P(DEAEMA30-co-PEGMA7)-b-PHPMA at 16.4% w/w HPMA concentration by systematic variation of ionic strength and pH value. (b) DLS particle size distributions obtained for the same series of diblock copolymer and (c) the corresponding TEM images. All HPMA monomer conversions > 95%.

considered equivalent to making it shorter, causing a subtle increase in the geometric packing parameter (P) towards higher order morphologies.[30]

Effect of hydrophobic block length on morphology.

In order to obtain higher order morphologies such as vesicles (*i.e.* beyond rods), a shorter macroRAFT agent was used: P(DEAEMA$_{30}$-*stat*-PEGMA$_7$). The target PHPMA DP$_n$ was varied between 250 and 450, and polymerizations were again conducted at 16.4% w/w monomer in the presence of 0.6 M NaCl. The MWDs (conversions > 95%) were narrow (D < 1.25) and shifted to higher molecular weights with increasing target DP$_n$ as expected (Fig. 2). TEM studies (Fig. 3a-3d) confirmed that a full range of morphologies was obtained, ranging from spheres to rods to vesicles, with relatively low DLS polydispersities (Fig. 3). An increase in DP$_n$ of the second

block leads to morphology transitions in the order spheres-rods-vesicles as well established in previous work.[6]

Morphology diagram.

A series of polymerizations were conducted using P(DEAEMA$_{30}$-*stat*-PEGMA$_7$) with a PHPMA target DP$_n$ of 450 at full conversion at various pH values and ionic strengths. The ionic strength (μ) was determined by $\mu = [Na^+] + [Cl^-] + [H^+]$,[48] where $[Na^+]$ is dictated by the NaCl concentration, whereas $[Cl^-]$ is influenced by both the NaCl concentration and the amount of HCl added to adjust the pH. The MWDs without NaCl addition at pH = 3-7 are shown in Fig. S2, revealing a high degree of control. Similar MWDs were obtained in all experiments performed with different pH and ionic strength since the degree of polymerization was the same.

At low ionic strengths, only spherical particles are formed across the entire pH range investigated. In the absence of NaCl, small spherical particles (~60 nm) with a rather polydisperse size distribution (DLS *PDI* ≈ 0.13) were obtained (Fig. 4a and 4b). This is because strong repulsive electrostatic forces between neighbouring stabilizer chains in the coronal layer hinder efficient self-assembly. In the presence of 0.10 M NaCl (Fig. 4c and 4d), corresponding to an ionic strength of 0.121 M, larger diameter nanoparticles (~80 nm) are formed. As the ionic strength is increased to 0.221 M at pH = 6, worm-like micelles start to form. At the same pH, pure rods are obtained at 0.321 M ionic strength, and when the ionic strength reaches 0.421 M, mainly vesicles but also a small amount of rods form. When the ionic strength was as high as 0.52 M, the morphologies do not change significantly with pH, but yields mixtures of vesicles/rods at all pH values investigated. However, increasing the ionic strength further by adding 0.6 M NaCl (pH = 7; Fig. 3d) results in formation of pure vesicles. The general trends seen in this morphology diagram conforms to the explanations provided above, whereby the formation of higher order morphologies is favoured by high pH and high ionic strength. The TEM images (Fig. 4a, 4c and 5c) corresponding to the phase diagram (Fig. 5a) are in good agreement with the intensity size data obtained by DLS (Fig. 5b).

Conclusions

Detailed investigations have been carried out on RAFT PISA dispersion polymerization of 2-hydroxypropyl methacrylate (HPMA) in water/methanol at 60 °C using the cationically charged macroRAFT agent P(*N,N*-diethylaminoethyl methacrylate)-*stat*-poly((ethylene glycol) methyl ether methacrylate) (PDEAEMA-*stat*-PEGMA). Using this macroRAFT agent, which has an LCST of 45 °C in water (Fig. S3), dispersion polymerization can only be performed if the pH is sufficiently low such that the stabilizer block is appropriately protonated to ensure solubility in the continuous phase. The non-charged monomer PEGMA was used as comonomer in the macroRAFT in order to reduce the charge density and enable formation of higher order morphologies. It has been demonstrated that morphologies ranging from spheres to rods to vesicles can be conveniently accessed by tuning of the pH (adjustment of HCl concentration) and the ionic strength (adjustment of the NaCl concentration) of the system. Higher order morphologies have a lower interfacial core/corona curvature, which leads to less charge separation and greater repulsive forces between the coronal chains. As such, an increase in pH (less protonation of DEAEMA units) and/or an increase in ionic strength (more charge screening) results in a shift towards higher order morphologies. In the present case, the morphology does not change significantly with pH variation when the ionic strength exceeds 0.52 M.

Overall, the present results illustrate how this system conveniently lends itself to tuning of the particle morphology, for a given recipe, by adjustment of the experimental parameters of pH and ionic strength.

Notes and references

1. W.-M. Wan, C.-Y. Hong and C.-Y. Pan, *Chem. Commun.*, 2009, DOI: 10.1039/B912804B, 5883-5885.
2. J. T. Sun, C. Y. Hong and C. Y. Pan, *Soft Matter*, 2012, **8**, 7753-7767.
3. B. Karagoz, L. Esser, H. T. Duong, J. S. Basuki, C. Boyer and T. P. Davis, *Polym. Chem.*, 2014, **5**, 350-355.
4. N. J. Warren and S. P. Armes, *J. Am. Chem. Soc.*, 2014, **136**, 10174-10185.
5. S. Dong, W. Zhao, F. P. Lucien, S. Perrier and P. B. Zetterlund, *Polym. Chem.*, 2015, **6**, 2249-2254.
6. S. L. Canning, G. N. Smith and S. P. Armes, *Macromolecules*, 2016, **49**, 1985-2001.
7. J. Yeow, O. R. Sugita and C. Boyer, *ACS Macro Lett.*, 2016, **5**, 558-564.
8. J. Yeow, J. Xu and C. Boyer, *ACS Macro Lett.*, 2015, **4**, 984-990.
9. P. B. Zetterlund, S. C. Thickett, S. Perrier, E. Bourgeat-Lami and M. Lansalot, *Chem. Rev.*, 2015, **115**, 9745-9800.
10. L. Zhang and A. Eisenberg, *Science*, 1995, **268**, 1728-1731.
11. L. Zhang and A. Eisenberg, *Macromolecules*, 1996, **29**, 8805-8815.
12. L. Zhang and A. Eisenberg, *Polym. Adv. Techn.*, 1998, **9**, 677-699.
13. D. E. Discher and A. Eisenberg, *Science*, 2002, **297**, 967-973.
14. Y. Mai and A. Eisenberg, *Chem. Soc. Rev.*, 2012, **41**, 5969-5985.
15. S. Boisse, J. Rieger, K. Belal, A. Di-Cicco, P. Beaunier, M.-H. Li and B. Charleux, *Chem. Comm.*, 2010, **46**, 1950-1952.
16. S. Boissé, J. Rieger, G. Pembouong, P. Beaunier and B. Charleux, *Polym. Sci. A Polym. Chem.*, 2011, **49**, 3346-3354.
17. I. Chaduc, A. Crepet, O. Boyron, B. Charleux, F. D'Agosto and M. Lansalot, *Macromolecules*, 2013, **46**, 6013-6023.
18. I. Chaduc, W. Zhang, J. Rieger, M. Lansalot, F. D'Agosto and B. Charleux, *Macromol. Rapid Commun.*, 2011, **32**, 1270-1276.
19. W. Zhang, F. D'Agosto, O. Boyron, J. Rieger and B. Charleux, *Macromolecules*, 2011, **44**, 7584-7593.
20. W. Zhang, F. D'Agosto, O. Boyron, J. Rieger and B. Charleux, *Macromolecules*, 2012, **45**, 4075-4084.
21. W. Zhang, F. D'Agosto, P.-Y. Dugas, J. Rieger and B. Charleux, *Polymer*, 2013, **54**, 2011-2019.
22. X. Zhang, S. Boissé, C. Bui, P.-A. Albouy, A. Brûlet, M.-H. Li, J. Rieger and B. Charleux, *Soft Matter*, 2012, **8**, 1130-1141.
23. X. Zhang, S. Boissé, W. Zhang, P. Beaunier, F. D'Agosto, J. Rieger and B. Charleux, *Macromolecules*, 2011, **44**, 4149-4158.
24. A. Blanazs, J. Madsen, G. Battaglia, A. J. Ryan and S. P. Armes, *J. Am. Chem. Soc.*, 2011, **133**, 16581-16587.
25. M. Semsarilar, V. Ladmiral, A. Blanazs and S. Armes, *Langmuir*, 2011, **28**, 914-922.
26. A. Blanazs, A. Ryan and S. Armes, *Macromolecules*, 2012, **45**, 5099-5107.
27. P. Chambon, A. Blanazs, G. Battaglia and S. Armes, *Macromolecules*, 2012, **45**, 5081-5090.

28. M. Semsarilar, V. Ladmiral, A. Blanazs and S. Armes, *Langmuir*, 2012, **29**, 7416-7424.
29. S. Sugihara, A. Blanazs, S. P. Armes, A. J. Ryan and A. L. Lewis, *J. Am. Chem. Soc.*, 2011, **133**, 15707-15713.
30. E. R. Jones, M. Semsarilar, A. Blanazs and S. P. Armes, *Macromolecules*, 2012, **45**, 5091-5098.
31. W. Zhao, G. Gody, S. M. Dong, P. B. Zetterlund and S. Perrier, *Polym. Chem.*, 2014, **5**, 6990-7003.
32. X. Zhang, J. Rieger and B. Charleux, *Polym. Chem.*, 2012, **3**, 1502-1509.
33. L. Zhang and A. Eisenberg, *Macromolecules*, 1996, **29**, 8805-8815.
34. M. Williams, N. J. W. Penfold and S. P. Armes, *Polym. Chem.*, 2016, **7**, 384-393.
35. S. M. Dong, W. Zhao, F. P. Lucien, S. Perrier and P. B. Zetterlund, *Polym. Chem.*, 2015, **6**, 2249-2254.
36. M. Williams, N. Penfold, J. Lovett, N. Warren, C. Douglas, N. Doroshenko, P. Verstraete, J. Smets and S. Armes, *Polym. Chem.*, 2016, **7**, 3864-3873.
37. M. Semsarilar, N. J. Penfold, E. R. Jones and S. P. Armes, *Polym. Chem.*, 2015, **6**, 1751-1757.
38. L. Carlsson, A. Fall, I. Chaduc, L. Wågberg, B. Charleux, E. Malmström, F. D'Agosto, M. Lansalot and A. Carlmark, *Polym. Chem.*, 2014, **5**, 6076-6086.
39. Y. Ning, L. A. Fielding, L. P. Ratcliffe, Y.-W. Wang, F. C. Meldrum and S. P. Armes, *J. Am. Chem. Soc.*, 2016, **138**, 11734-11742.
40. Y. Ning, L. Fielding, T. Andrews, D. Growney and S. Armes, *Nanoscale*, 2015, **7**, 6691-6702.
41. V. Ladmiral, A. Charlot, M. Semsarilar and S. P. Armes, *Polymer Chemistry*, 2015, **6**, 1805-1816.
42. K. E. Doncom, A. Pitto-Barry, H. Willcock, A. Lu, B. E. McKenzie, N. Kirby and R. K. O'Reilly, *Soft matter*, 2015, **11**, 3666-3676.
43. P. Van de Wetering, N. Zuidam, M. Van Steenbergen, O. Van der Houwen, W. Underberg and W. Hennink, *Macromolecules*, 1998, **31**, 8063-8068.
44. A. Darabi, P. G. Jessop and M. F. Cunningham, *Macromolecules*, 2015, **48**, 1952-1958.
45. A. Darabi, A. R. Shirin-Abadi, P. G. Jessop and M. F. Cunningham, *Macromolecules*, 2014, **48**, 72-80.
46. A. Darabi, A. R. Shirin-Abadi, J. Pinaud, P. G. Jessop and M. F. Cunningham, *Polym. Chem.*, 2014, **5**, 6163-6170.
47. Y. Y. Mai and A. Eisenberg, *Chem. Soc. Rev.*, 2012, **41**, 5969-5985.
48. P. Atkins and J. d. Paula, *Atkins' Physical Chemistry*, Oxford University Press, 10th edn., 2014.